Energy Harvesting-Based Vibration Sensor for Medical Electromyography Device

Mustafa F. Mahmood, Saleem Lateef Mohammed, and Sadik Kamel Gharghan
Department of Medical Instrumentation Techniques Engineering, Electrical Engineering Technical College, Middle Technical University, Baghdad, Iraq
Email: musiraq86@gmail.com; saleem_lateef_mohammed@mtu.edu.iq; sadik.gharghan@ mtu.edu.iq

Abstract—**Many wearable or portable medical devices have limited battery energy. In this paper, a piezoelectric transducer (PZT) was adopted to take advantage of bodyweight to generate power to wearable and implantable medical devices. To confirm the power generated by the PZT, electromyography (EMG) was used to measure the subject's muscle activity. The proposed system consists of three parts: power, measurement, and monitoring units. The power unit was tested using on 0.25 F, 0.33 F, 0.5 F, and 1 F supercapacitors to explore the best supercapacitor that can supply the measurement unit by power. Based on using PZT, we found that the power unit was able to supply the measurement unit with adequate voltage (i.e., 5 V) for normal operation without system failure. The present system has better performance than state-of-the-art in terms of power and voltage as compared to that in previous studies.**

Index Terms—**Arduino, DC-DC converter, MyoWare muscle sensor, nRF24L01, piezoelectric transducer, supercapacitors**

I. Introduction

Modern-day technologies provide the global community with a sustainable environment and a future without power interruption. There are various sources of free power, such as biomass, solar, radiofrequency, wind, water, and heat. Researchers have focused on studying piezoelectricity to produce power for operating medical sensors and implantable biomedical devices (IBDs), for example, glucose meters, electrocardiograms (ECG), oximeters, heart rate monitors, and electromyography sensors (EMG), which are frequently used to obtain a better quality of life for those who are ill [1], [2]. Piezoelectricity generates a voltage directly when stress and pressure are applied [3]. Examples of piezoelectric materials are lead titanate, quartz, and topaz. Solid particle charges are arranged randomly, such that the net electric dipole moment is null. When force is applied to piezoelectric materials, the positive and negative particles accumulate at two extremities to form a potential difference between the two charged surfaces. It is a solution to the wasteful problem of power shortage. Not only does it increase the electricity generated, it also supplies any device with an immediate power-generating source [4]. Piezoelectricity does not lead to any pollution or damage its surroundings [4], [5]. This presents the possibility of using materials with piezoelectric properties to treat diseases via innate piezoelectricity for improving organ function, as these properties are present in the human body, being contained in the blood vessels, bone, and skin [6]. Piezoelectricity has been used in mechanical applications, e.g., car suspensions, to yield real energy value [7]. To optimize an implantable medical device (IMD), several investigators [8] have used piezo-electricity to generate power in wearable biomedical devices and IMDs such as heart rate monitors. Additional components, such as MOSFET (metal oxide-silicon field-effect transistor) bridge rectifiers consisting of two n-channels and two p-channels, are used in IMDs to improve power [9]. In [10], a special-design piezoelectric transducer (PZT), such as a piezoelectric polymer polyvinylidene fluoride-trifluoroethylene, was used to optimize power for operating a medical sensor. One group reported using a storage capacitor or a battery-free device to operate medical devices [11]. Other researchers have used program simulations to design PZT, which were implanted, and suitable force was applied to the sensor to produce adequate power. Programs such as MATLAB, COMSOL Multiphysics, CoventorWare simulation, OpenSim modeling software, and ANSYS software have been used to calculate voltage and power in open and closed circuits [12]-[19], respectively. Others [20]-[22] have used PZT to study voltage in open circuits and to connect elements for wearable, battery-free sensors in the future.

Here, the proposed system comprises three main parts: power unit, measurement unit, and monitoring unit. The power unit includes a 12-piece PZT, a bridge rectifier, a boost converter (DC-DC), and supercapacitors. The measurement unit comprises a MyoWare sensor-based EMG sensor, a microcontroller based-Arduino Nano, and a wireless protocol transmitter (nRF24L01) for sending data from the measurement unit to the monitoring unit. The monitoring unit includes an nRF24L01 module, a microcontroller based-Arduino Mega 2560, and a monitoring device such as a laptop/notepad to display EMG measurements using MakerPlot data acquisition software. The main objective of the present study was to generate power to supply a battery-free measurement unit.

Manuscript received November 19, 2019; revised January 2, 2020; accepted January 16, 2020.

Corresponding author: Mustafa F. Mahmood (email: musiraq86@ gmail.com).

©2020 Int. J. Elec. & Elecn. Eng. & Telcomm.

doi: 10.18178/ijeetc.9.5.364-372

The contributions of this study are highlighted as follows:

- Design and implementation of lightweight piezoelectric transducer prototype to supply the measurement unit (which includes wearable electromyography (EMG) sensor, microcontroller based-Arduino Nano, and nRF24L01 module) by an adequate power.
- Several supercapacitors have been experimentally tested to explore the best one that can be used to supply the measurement unit with power within an appropriate time.
- The data of the EMG sensor were successfully transmitted from the measurement unit to the monitoring unit using generated power by a piezoelectric transducer in the power unit.
- The power generated by the power unit outperformed the state-of-the-art.

The rest of the paper includes the following: Section II, which discusses previous studies related to power generated using PZT. Section III introduces a proposed PZT design. Section IV introduces the experimental configuration of the PZT. Section V presents the results and discussion of the PZT system. Section VI compares the results of the proposed system with that of related studies. Finally, Section VII presents the conclusion and future works.

II. Related Works

This partition highlights related works uses a piezoelectric transducers for generating energy at vital sign monitoring systems for the patient. Ansari *et al*. [8] designed and implemented a piezoelectric sensor for wearable biomedical devices and implantable devices such as heart rate monitors. The system operated at a frequency of <20 Hz and included a piezo element, supercapacitor, and device. The researchers used two categories of piezoelectric transducers in their experiments. The experimental results revealed that using small-scale rather than large-scale piezoelectrics generated greater power at 16 μW at 18.4 g. The design has some advantages, for instance, a wearable device, small-size, and cheap. Nevertheless, the system itself is large. Taeho *et al*. [9] designed and used vibrations in wearable sensors to produce voltage based on the piezoelectric element. The system included the piezoelectric element, rectifier, regulator, and wearable sensors. Experimental outcomes divulged that an output power was 10.7 μW using a MOSFET bridge rectifier consisting of two n-channels and two p-channels. The output and input voltage was 694 mV and 703 mV at 45 kΩ load, respectively. The design has some advantages, for instance, a small-size, a wearable device, and inexpensive. Nevertheless, the system itself is large. Toprak *et al*. [10] designed and implemented a vibration-based PZT to generate power for a wearable sensor. The system operated at a frequency of 1.74 kHz. The system included piezoelectric polymer polyvinylidene fluoride-trifluoroethylene energy harvesters and buffer circuit. Experimental outcomes divulged that a maximum produces was 35 pW and 33.3 mV, respectively, at 4.3 MΩ, with high displacement. The system has several advantages: lightweight, low power consumption, and low cost. Nonetheless, it has low power.

Zhang *et al*. [11] presented a vibration-based harvesting technique using a piezoelectric sensor for a wearable device. The system operated at frequencies between 100 Hz to 170 Hz. It is included piezoelectrics material, rectifier, and the storage capacitor. Experimental outcomes divulged that a produce power was 2.22 μW at 160 Hz at acceleration 10.5 m/s^2. It has some advantages, for instance, small-size, a wearable device, and inexpensive. Nonetheless, it had a limited amplitude. Janusas *et al*. [12] presented a wearable device using vibration-based on piezoelectric material to generate power. The system operated at a frequency of 50 Hz and included a piezoelectric sensor and load. The experimental results showed up to 80 μV output voltage. The design has some advantages, for instance small-size, inexpensive, and easy to design. Nonetheless, the design has prototype. Saadon *et al*. [13] designed and implemented vibration-based piezoelectric plates to generate power for different applications such as wearable sensors. The system operated at a frequency of 67 Hz to 70 Hz and used the CoventorWare simulation program to study the output power and voltage at acceleration. The experimental results revealed that the produces were 6.8 μW with 0.4 V when applying a force with a weight of 0.2 g to 1.3 g at 20 kΩ. The system has several advantages: lightweight, consumption a low-power, and inexpensive. Nonetheless, the design has prototype. Safaei *et al*. [14] implemented a vibration-based PZT in knee implants to generate power for a wearable device. The system operated at a frequency of 25 Hz and used OpenSim modeling software, ANSYS software, and MATLAB software to simulate a knee, design a PZT, and calculate the power and voltage. Experimental outcomes divulged that a produces were 12 μW and 2.3 V at 1 MΩ load. The system has several advantages: lightweight, consumption at low-power, and cheap. Nonetheless, the system has prototype.

Pillatsch *et al*. [15] reported on vibration-based piezoelectricity for generating power for a wearable device. The system operated at a frequency of 0.5 Hz to 4 Hz and contained piezoelectric materials and load. The experiment used five accelerations. The experimental results showed that the output power was high at high acceleration. The output power was 20 μW at 2 Hz with acceleration 20 m/s^2. A maximum output voltage at 150 kΩ load was 12 V. The design has some advantages for instance wearable device, inexpensive, and small-size. However, the system has a prototype. Ghosh *et al*. [16] presented a vibration-based piezoelectric element to generate power for a wearable device. The system operated at a frequency of 0.1 kHz to 1000 kHz and contained a piezoelectric element, rectifier, and device. The experiential outcomes showed that a harvest term in current and voltage the closed-circuit was 1.5 μA with 4 V. in addition, maximum energy was 1.14 μW; the power at 13 MΩ was 0.47 μW. The design has some advantages for instance inexpensive, small-size, and a wearable device. However, the system has prototype.

Yu *et al*. [17] presented a vibration-based harvesting technique using a piezoelectric sensor to generate power for a wearable device. The system operated at frequencies between 180 Hz to 230 Hz and included piezoelectrics material and load. The experimental results obtained via the COMSOL program revealed that the output power was 1.78 μW at 210 Hz with acceleration 0.6 m/s^2. The output power increased with acceleration. The design has some advantages, for instance, small-size, inexpensive, and wearable device. Nevertheless, the design has a prototype. Won *et al*. [18] presented a vibration-based piezoelectric element to generate voltage for a wearable device. The system operated at a frequency of 0.25 Hz to 1 Hz and contained a piezoelectric element and load. Two circuits were used in experiments at different frequencies. The experiential outcomes showed that a harvest voltage for the system was 1.5 V with 0.38 μA at 1 Hz, whereas it was 0.4 V at 0.25 Hz when using piezoelectric poly (vinylidene fluoride trifluoroethylene). The design has some advantage for instance inexpensive, small-size, and wearable device. However, the design has prototype.

Parali *et al*. [19] reported on vibration-based piezoelectricity for generating different frequencies and displacements for a laser device. The system was operated at a frequency of 0.01 Hz to 20000 kHz and comprised two parts: a hardware part involving the piezoelectric material, power amplifier, and load; a second part using MATLAB and LabVIEW. The experimental results revealed that in converting from a mechanical to electrical model, the displacement for excitation at 3 V was greater than 0.5 V. The frequency with displacement at 3 V and 0.5 V was 7 kHz with 1.21 μm and 6.9 kHz with 0.261 μm, respectively. The design has some advantages, for instance, a wearable device, inexpensive, and consumption low-power. However, the system has a prototype. Youfan *et al*. [20] reported on vibration-based harvesting using a piezoelectric sensor to generate power for a wearable device at low frequency. The system included the piezoelectric material, rectifier, storage unit, and load. The experimental results using skin near the human eye revealed that the harvest voltages at open circuit was 37 V, whereas the output current of the short circuit was 0.6 μA. The design has some system has some advantages for instance small-size, a wearable device, and inexpensive. Nevertheless, the system has low-current.

Kim *et al*. [21] presented a vibration-based harvesting technique using a piezoelectric sensor for a wearable device. The system operated at a frequency of 0.1 kHz to 100 kHz and included the piezoelectric material and load. The experimental results revealed that the biocompatible (Na0.5K0.5)-NbO3 film–based on a nanogenerator had a large the produced voltage at open-circuit was 2.0 V, whereas production current at short-circuiting was 40 nA. The design has some advantage, for instance, small-size, a wearable device, and cheap. Nevertheless, the voltage of the system has an effect on temperature. Bingwei *et al*. [22] reported on vibration-based piezoelectricity for implantable medical devices such as pacemakers to generate power at low frequency. The system consisted of a piezoelectric element, rectifier, battery, and load. The experiment was conducted on pigs, where the device was implanted in the chest. Experimental outcomes revealed that a production voltage was 3 V_{pp} when using piezo-electric LZT. The design has some advantage, for instance, a wearable device, small-size, and cheap. Nevertheless, the batteries were affected by the environment and had to be replaced.

Here, we obtained high power based on PZT for charging yield supercapacitors to obtain adequate power at different times. This power is optimized compared with that of the previous studies. The supercapacitors supplied an Arduino Nano microcontroller, MMS, and nRF24L01 wireless protocol with adequate power. Data were exchanged between the measurement and monitoring units using the wireless protocol. Table I summarizes a previous studies and compares their performance metrics such as operation frequencies, voltages, powers, circuit type, and weight at different references.

TABLE I: PERFORMANCE A-METRICS FOR THE LITERATURE SURVEY STUDIES.

Refs	Objectives	Operation frequencies (kHz)	Harvesting-techniques	Implementation-environments	Applications	Voltage (V)	Power (μW)	Circuit type (kΩ)
[8]	Generate power	0.02	PZT	Experimental	Heart rate	-------	16	Closed
[9]	Generate power	0.2	PZT	Experimental	Wearable sensor	0.694–0.703	10.7	45
[10]	Generate voltage	1.074	PZT	Experimental	Wearable device	0.0108	0.018	1000
[11]	Generate power	0.160	PZT	Experimental	Wearable device	-------	2.22	Closed
[12]	Generate voltage	0.05	PZT	Simulation	Wearable device	8 × 10-5	-------	Closed
[13]	Generate voltage	0.067–0.070	PZT	Simulation	Wearable device	0.4	6.8	20
[14]	Generate voltage	0.025	PZT	Simulation	Knee/wearable device	2.3	12	1000
[15]	Generate power	0.002	PZT	Simulation	Wearable device	12	20	150
[16]	Generate power	0.1–1000	PZT	Simulation	Wearable device	4	0.47	Closed
[17]	Generate power	0.21	PZT	Simulation	Wearable device	-------	1.78	Closed
[18]	Generate voltage	0.00025–0.1	PZT	Simulation	Wearable device	1.5	-------	Open
[19]	Generate voltage	0.01–20000	PZT	Simulation	Wearable device	3	-------	Open
[20]	Generate voltage	-------	PZT	Experimental	Wearable device	37	-------	Open
[21]	Generate voltage	0.0001–0.1	PZT	Experimental	Wearable sensor	2	-------	Open
[22]	Generate voltage	-------	PZT	Experimental	Wearable device	3	-------	Open

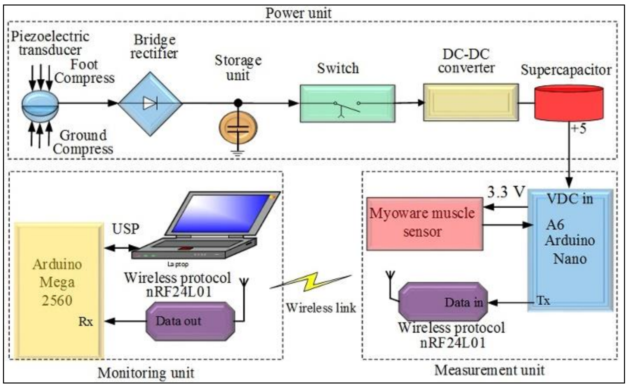

Fig. 1. Block diagram of the use of a PZT for an EMG sensor.

III. System Model

The proposed PZT Fig. 1 involved the power, monitoring, and measurement units. The power unit contains the PZT, bridge rectifier, ON/OFF switch, DC-DC converter, and supercapacitor. The PZT converts mechanical signals to electrical signals; the generated signal is an alternate signal. The bridge rectifier converts the AC signal to DC. The switch is used to switch the system between the ON-OFF states. The boost converter is a DC-DC converter (MT3608 module, 36 mm ×17 mm ×14 mm). The converter has a conversion efficiency of >93%, and it is cheap and small [23].

The measurement unit consists of a microcontroller based-Arduino Nano, EMG sensor, and nRF24L01 module. The monitoring unit comprises a microcontroller based-Arduino Mega 2560, nRF24L01 module, and a laptop. The microcontroller based-Arduino Nano is small, inexpensive, lightweight, programmed using C++ language, and targeted at low power consumption [24]-[26]. The EMG sensor is analog, inexpensive, and lightweight [27], [28]. The nRF24L01 module is low-energy, cheap, lightweight, and can transmit data up to 100 m between two nodes in an outdoor environment [29], [30]. In addition, the nRF24L01 module uses a radio frequency of 2.4 GHz. The nRF24L01 module has several applications, for example, wireless computer accessories, wireless information communication, engineering sensor, and as a sensor network in ultra-low power sensor networks. The nRF24L01 protocol is robust because it has the following advantages: the transmitted power can be modified to 0 dBm, −6 dBm, −12 dBm, and −18 dBm with current consumption of 11.3 mA, 9 mA, 7.5 mA, and 7 mA, respectively; the data rate can be configured to 1 Mbps and 2 Mbps and 250 kbps, there is configurable packet length size; it can interface with low-power 4-bit or 8-bit microcontrollers; it features error detection and retries for securing and receiving data [31], [32]; and it has frequency aimed at guaranteeing communication between nRF24L01 devices in the presence of interference from other wireless technology such as Bluetooth, ZigBee, and Wi-Fi [33].

The monitoring unit uses a microcontroller based-Arduino Mega 2560, nRF24L01 module, and a laptop. The microcontroller is lightweight, inexpensive, and programmed using C++ language [34]. The wireless protocol is as described above. The laptop is used to display the results via MakerPlot. Fig. 2 illustrates the hardware of the measurement unit. The supercapacitor is connected to the supply voltage pins of the Arduino Nano platform (VIN and GND). Hence, the EMG sensor and nRF24L01 are connected to the +3.3 V pin of the microcontroller and the ground pin. In addition, the output signal of the EMG sensor is joined to the A0 pin of the microcontroller. The nRF24L01 pins (i.e., D7, D8, D13, D11, and D12) are linked to the microcontroller for data transmission

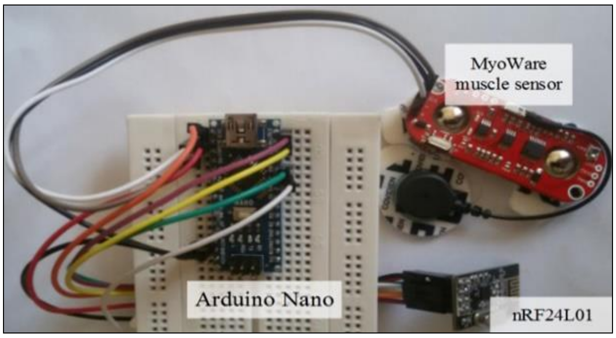

Fig. 2. Circuit diagram of the EMG and the wireless protocol.

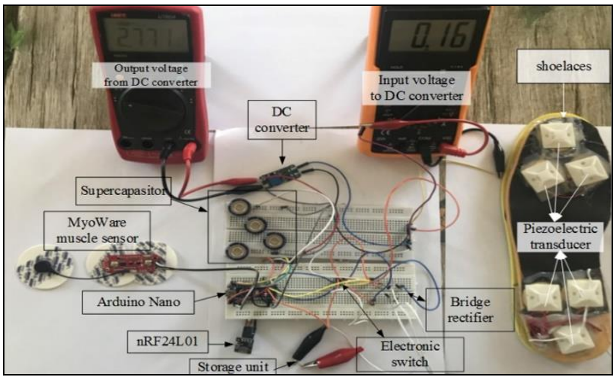

Fig. 3. Circuit diagram based on PZT system circuit.

IV. Experiment Configuration

The piezoelectric ceramic transducer features a 35-mm diameter copper piece [35]. Fig. 3 shows the circuit diagrams of the whole system. First, the 12-piece PZT was implanted up and down the shoelaces. The pieces were connected in parallel to increase the current value. The PZT converts a mechanical signal to an electrical signal at a low frequency of less than 3 Hz based on the force applied. Second, AC was converted to DC using the bridge rectifier; a Schottky diode (model SR260) [36] was used because of the low voltage drop, which was about 0.18 V. Third, we used a capacitor to filter the noise in the voltage signal from the bridge rectifier, which was about 100 nF at 50 V. Fourth, the supercapacitor was charged when the electronic ON-OFF switch was closed. Next, the DC-DC converter was used to increase the low output voltage from 1.8 V to 4.2 V. The converter output (i.e., 4.2 V) was applied to the supercapacitor to obtain 5 V, which in turn could be used to supply power to the measurement unit. We tested 0.25 F, 0.33 F, 0.5 V, and 1 F supercapacitors to select the capacitor that would yield a higher output voltage with

©2020 Int. J. Elec. & Elecn. Eng. & Telcomm.

shorter charging time. Consequently, the 0.25 F supercapacitor was selected. The mechanism for charging supercapacitors within a specific time was governed by

$$V_c = V_s\left(1-e^{-t/\tau}\right) \tag{1}$$

$$I_c = I_s\left(1-e^{-t/\tau}\right) \tag{2}$$

$$\tau = RC \tag{3}$$

where V_c and I_c are the voltage and current, respectively, at a specific time. V_s and I_s are the voltage and current, respectively, at the source; τ is a constant for time, R is a resistor, and finally, C is a capacitor.

A 10 Ω resistor was connected in series with the supercapacitor to obtain a shorter charging time (Equation (3)) [37], [38].

Fig. 4 demonstrates a snapshot of the PZT-based system on calf muscles for generating adequate voltage to operate a wearable device. Fig. 4 (a) illustrates the installation of the measurement unit on the gastrocnemius muscle of the subject's left leg. Fig. 4 (b) shows the measurement unit connected to the soleus muscle at the end of the subject's right leg. However, the generated power mainly depends on the user's weight. The measurement unit transmits the EMG sensor data to the monitoring unit through the nRF24L01 module. The nRF24L01 module of the monitoring unit receives the data and sends it to the Arduino Mega platform via USB connection for processing and for viewing on the laptop.

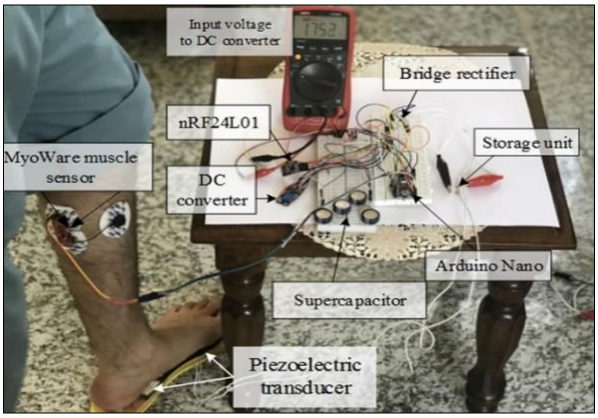

(a)

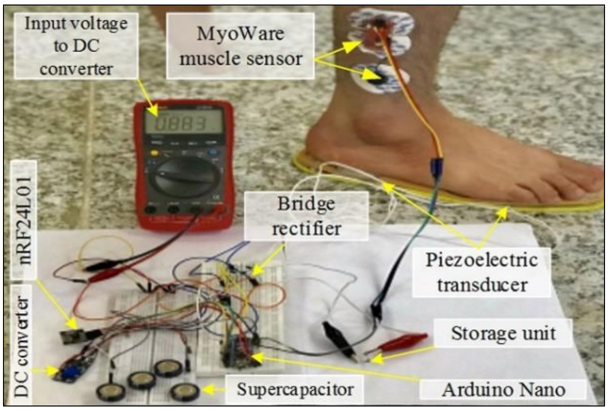

(b)

Fig. 4. Snapshot of PZT-based system for calf muscles: (a) gastrocnemius and (b) soleus.

V. Results and Discussion

A. Supercapacitor Charging

Fig. 5 shows the voltage values for the 0.25 F, 0.33 F, 0.5 F, and 1 F supercapacitors with respect to charging time. The *x*-axis indicates the time (min); the *y*-axis indicates the output voltage of the supercapacitors (V). The full charging time for the 0.25 F, 0.33 F, 0.5 F, and 1 F supercapacitors was 41 min, 61 min, 154 min, and 295 min, respectively, based on real measurements corresponding with (1), (2), and (3). The results show that the 0.25 F supercapacitor yielded the best output voltage for supplying power to the microcontroller, which in turn supplied the MyoWare muscle sensor and the nRF24L01 module of the measurement unit. By contrast, the 1 F supercapacitor performed the poorest because it required 295-min charging time. The charging times of the 0.33 and 0.5 F supercapacitors were between that of the above two supercapacitors. Fig. 5 illustrates the minimum voltage (i.e., 2.7 V) at which the measurement unit could be operated without system degradation.

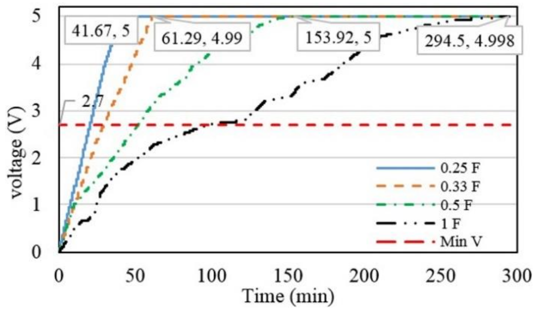

Fig. 5. Supercapacitor charging categories by time.

B. Performance Metrics According to Load

Several experiments were conducted to calculate the output power and voltage at different loads based on the PZT Fig. 6. In Fig. 6 (a), the *x-axis* indicates the resistance load (kΩ); the *y-axis* shows the output power obtained from the DC-DC converter (μW). We selected a yield load of 0.33–1500 kΩ Fig. 6 (a). Maximum power of 197 μW was recorded at 15 kΩ, whereas the minimum power was 18 μW and 27 μW at 330 kΩ and 1.5 MΩ, respectively. Clearly, the output power decreased as the resistive load increased, and vice versa. In Fig. 6 (b), the *x-axis* indicates the resistance load (kΩ); the left *y-axis* represents the DC output voltage (V) of the DC-DC converter; the right *y-axis* displays the current (μA). The orange circle line indicates the current (μA). The maximum value was 207 μA at 470 Ω, and the minimum value was 3 μA at 1.5 MΩ. It is clear that the current was decreased as the load resistance increased. The blue square dotted line indicates the output voltage of the DC-DC converter (V): the maximum value was 9 V at 1.5 MΩ, and the minimum value was 0.1 V at 330 kΩ. The output voltage (i.e., 8 V) increased slightly after 390 kΩ until it was 9 V at 1.5 MΩ. However, the supercapacitor required 4.2 V for charging. This means that the output voltage of the DC-DC converter was adequate for charging the supercapacitor. It is worth mentioning that the power unit was tested experimentally in an open-loop circuit, where the output voltage was 40 V.

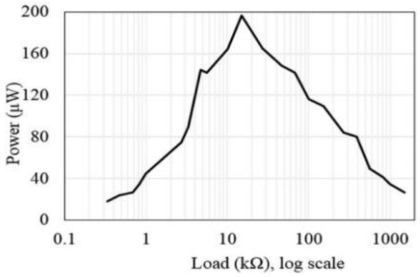

(a)

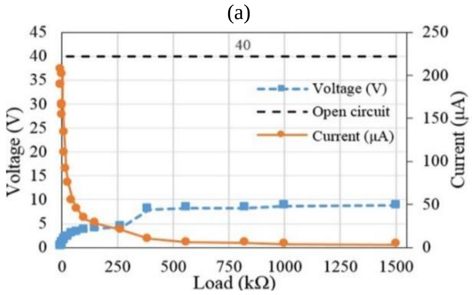

(b)

Fig. 6. PZT-based parameters at loads: (a) power, (b) voltage and current.

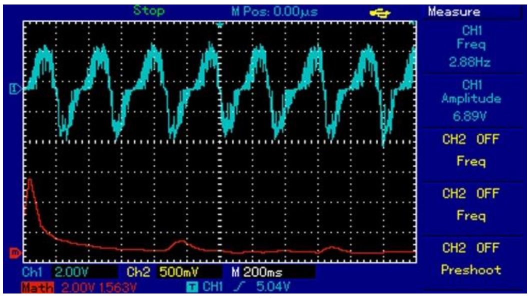

(a)

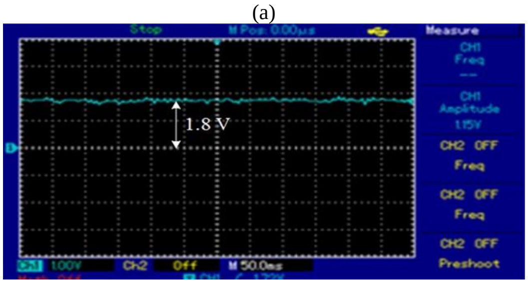

(b)

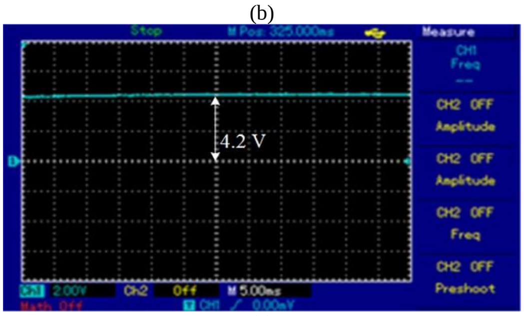

(c)

Fig. 7. The waves of the system: (a) PZT input wave, (b) input wave of the DC boost converter, and (c) output wave of the DC boost converter.

C. PZT-Based Voltage Signals

Under the experimental arrangement, the voltage signal and spectrum for analyses were visualized using a PZT-based storage oscilloscope (model UTD2025CL). In Fig. 7 (a), the blue waveform is the output voltage of the PZT; the red line is the frequency spectrum of the signal generated from the PZT. The input voltage based-PZT was observed as a distorted sinusoidal wave with an amplitude of 7 Vpp (peak-peak voltage) at a low frequency of 2.88 Hz (waveform in Fig. 7 (a)). The signal was converted from AC to DC by utilizing the bridge rectifier to produce 1.8 V (Fig. 7 (b)). This voltage value was low, therefore it had to be boosted in the next step. The DC-DC converter was used to modify the 1.8 V to pure DC voltage of 4.2 V because it contains a DC filter (Fig. 7 (c)). This voltage value was adequate for charging the 0.25 F supercapacitor to yield 5 V. The 5 V was adequate voltage for operating the microcontroller, which in turn powered the EMG sensor and nRF24L01 module. The PZT-based power supply presented several advantages compared to direct connection (wire charging), such as: (i) it is a low-power device that does not require batteries, (ii) user movements are facilitated because movement is not obstructed by wires, (iii) the system is lightweight because it is battery-free, (iv) the design can be used in any location because it does not need a main AC source of electricity, and (v) different types of PZT can be implanted to power a medical device [14].

Fig. 8 depicts the voltage output for each part based on the PZT. First, the PZT was used to generate an alternating voltage of about 7 Vpp at 2.88 Hz according to the applied force on the PZT. Second, the AC was converted to 1.8 VDC voltage using a bridge rectifier. Third, this voltage was modified to 4.2 V using a DC-DC converter. Fourth, the final voltage (i.e., 4.2 V) was used to charge a 0.25 F supercapacitor to operate the measurement unit. Finally, the supercapacitor was used as a power source for the microcontroller based-Arduino Nano at 5 V. In addition, the microcontroller supplied the EMG sensor and nRF24L01 module with a 3.3 V voltage.

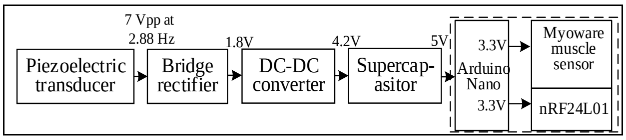

Fig. 8. Block diagram of PZT-based output voltage.

D. EMG Signal

The measurement unit measured the muscle activity and sends the data via the nRF24L01 module to the monitoring unit. A sensor was positioned in the leg (the calf muscle). The monitoring unit received data via wireless protocol (Fig. 9 (a)). The EMG signals for the gastrocnemius muscle (Fig. 9 (b)) and the soleus muscle (Fig. 9 (c)) were measured using MakerPlot version 1.6.0. The *x-axis* indicates the time (sec); the *y-axis* indicates muscle relaxation/contraction (peaks). The blue and red signals in Fig. 9 (b) and Fig. 9 (c) indicate the muscle activation for contraction (high value) and relaxation (low value), respectively. However, the amplitude of the signal depended on the gastrocnemius muscle activity. EMG was used to verify the proposed PZT design. We determined that the PZT could supply power to the measurement unit. Therefore, the EMG sensor can be used to measure muscle activity and fatigue when jogging, playing soccer or sports-related to walking or running, and rehabilitation without power failure.

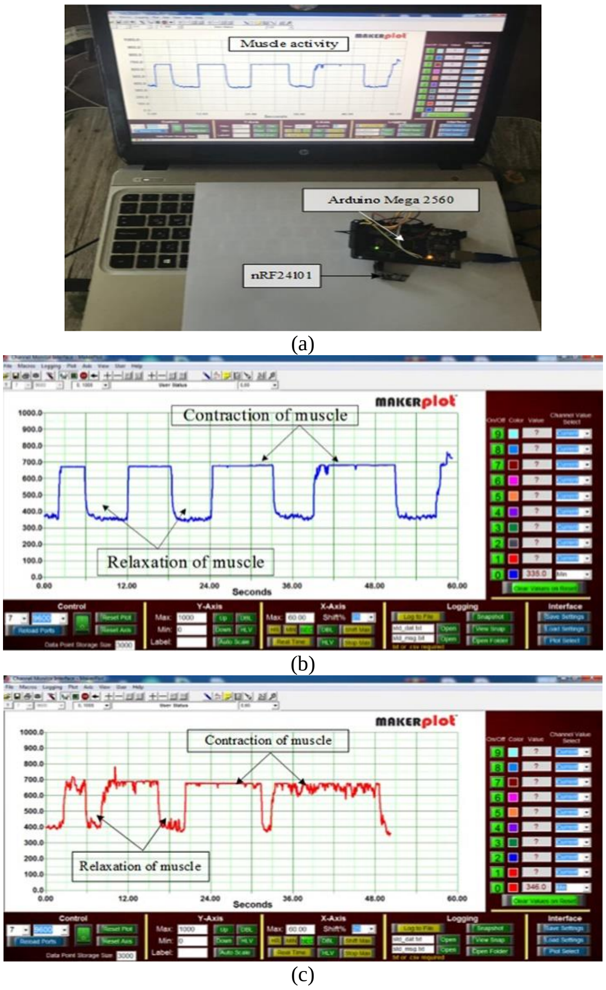

Fig. 9. Snapshot of the EMG measurements from MakerPlot: (a) monitoring unit, (b) gastrocnemius muscle, and (c) soleus muscle.

E. Comparison of Results

To validate the proposed PZT power system, the present work was compared to relate to previous studies. Fig. 10 compares the generated power in the present PZT with that of previous works at different loads. Here, the maximum power of the closed-circuit was 197 µW, whereas it was 16 µW and 20 µW in [8] and [15], respectively. The figure shows that the present proposed system outperforms the previously reported systems. Furthermore, Fig. 10 shows that the power in the present work was 180 µW, 140 µW, 110 µW, and 35 µW, whereas it was 6.8 µW [13], 10.7 µW [9], 20 µW [15], 0.035 µW [10], and 12 µW [14] at a resistive load of 20 kΩ, 45 kΩ, 150 kΩ, and 1000 kΩ, respectively. Table II compares the generated power based on PZT in the current research with other research according to parameters such as an operation frequency, implementation environments, application, the voltage generated, the power generated, and circuit type. The present PZT system has better performance than state-of-the-art in terms of generated power and voltage at different loads under testing as compared to that in previous studies.

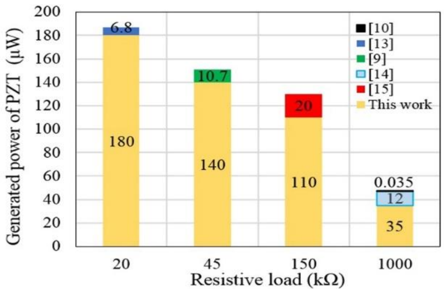

Fig. 10. Comparison of generated power between the present work and previous works for different loads.

TABLE II: COMPARISON OF POWER GENERATED BETWEEN THE CURRENT RESEARCH AND OTHER RESEARCHES

Refs	Operating frequency (kHz)	Implementation-environments	Type of sensor	Voltage (V)	Power (µW)	Circuit type (kΩ)
[8]	0.02	Experimental	Heart rate	N/A	16	Closed
[9]	0.2	Experimental	Wearable sensor	0.694–0.703	10.7	45
[10]	1.074	Experimental	Wearable device	0.0108	0.018	1000
[11]	0.160	Experimental	Wearable device	N/A	2.22	Closed
[13]	0.067–0.070	Simulation	Wearable device	0.4	6.8	20
[14]	0.025	Simulation	Knee/ wearable device	2.3	12	1000
[15]	0.002	Simulation	Wearable device	12	20	150
[16]	0.1–1000	Simulation	Wearable device	4	0.47	Closed
[17]	0.21	Simulation	Wearable device	N/A	1.78	Closed
Current work	0.00288	Experimental	EMG sensor	2	197	15

VI. CONCLUSIONS

We propose the design and implementation of a PZT for supplying low power to EMG sensors. A PZT power unit was examined by charging 0.25 F, 0.33 F, 0.5 F, and 1 F supercapacitors. These supercapacitors were evaluated to determine the capacitor value to be used in the system with respect to a fast charge time with good results for other capacitor values. The 0.25 F supercapacitor charged the design in 41 min. In addition, high power of 197 µW was generated at 15 kΩ. Furthermore, the high output voltage of the open circuit was 40 V. The obtained output voltage of the supercapacitor was 5 V. This voltage was adequate for supplying power to the microcontroller based-Arduino Nano, which in turn supplied power to the EMG sensor and nRF24L01 module. The PZT-based power generation was superior to that of previous studies. At different supercapacitor values, the capacitor charging time increased with supercapacitor capacity. Therefore, we recommend using the proposed low value, i.e., the 0.25 F supercapacitor, to obtain adequate voltage quickly. In the future, we will increase the amount of power generated based on the PZT, and decrease the supercapacitor charging time. Furthermore, a small microcontroller chip, e.g., the ATmega 328P, can be used in the measurement unit to reduce power consumption.

©2020 Int. J. Elec. & Elecn. Eng. & Telcomm.

Conflict of Interest

The authors declare no conflict of interest.

Author Contributions

Sadik Kamel Gharghan and Mustafa F. Mahmood conducted Data curation; Mustafa F. Mahmood conducted resource and formal analysis; Sadik Kamel Gharghan and Saleem Lateef Mohammed conducted the investigation; Mustafa F. Mahmood and Sadik Kamel Gharghan built the methodology; Saleem Lateef Mohammed and Sadik Kamel Gharghan conducted the supervision; Mustafa F. Mahmood conducted the visualization; Sadik Kamel Gharghan validated the results. The paper was written by Mustafa F. Mahmood and Saleem Lateef Mohammed, and reviewed by Sadik Kamel Gharghan and Mustafa F. Mahmood. All authors had approved the final version.

Acknowledgment

The author would like to thank the staff of the Department of Medical Instrumentation Techniques Engineering, Electrical Engineering Technical College, Middle Technical University for their support during this study.

References

[1] E. J. Curry, K. Ke, M. T. Chorsi, K. S. Wrobel, A. N. Miller, A. Patel, *et al.*, "Biodegradable piezoelectric force sensor," *Proceedings of the National Academy of Sciences*, vol. 115, no. 5, pp. 909-914, January 2018.

[2] X. Wang, Z. Liu, and T. Zhang, "Flexible sensing electronics for wearable/attachable health monitoring," *Small*, vol. 13, no. 13, p. 1602790, March 2017.

[3] F. C. P. Ulhôa, P. A. A. Magalhães, R. A. D. S. Floriano, and V. N. Coutinho, "Electric power generation with piezoelectricity for cargo ships," in *Proc. Twelfth Int. Conf. on Ecological Vehicles and Renewable Energies (EVER)*, June 2017, pp. 1-8.

[4] J. Chen, Q. Qiu, Y. Han, and D. Lau, "Piezoelectric materials for sustainable building structures: Fundamentals and applications," *Renewable and Sustainable Energy Reviews*, vol. 101, pp. 14-25, March 2019.

[5] M. Pohanka, "The piezoelectric biosensors: Principles and applications," *Int. J. Electrochem. Sci.*, vol. 12, pp. 496-506, January 2017.

[6] M. Chen-Glasser, P. Li, J. Ryu, and S. Hong, "Piezoelectric materials for medical applications," in *Piezoelectricity-Organic and Inorganic Materials and Applications*, IntechOpen London, 2018, pp. 125-145.

[7] B. Lafarge, S. Cagin, O. Curea, and A. H. Perret, "From functional analysis to energy harvesting system design: application to car suspension," *Int. Journal on Interactive Design and Manufacturing*, vol. 10, no. 1, pp. 37-50, February 2016.

[8] M. Ansari and M. A. Karami, "Experimental investigation of fan-folded piezoelectric energy harvesters for powering pacemakers," *Smart Materials and Structures*, vol. 26, no. 6, p. 065001, May 2017.

[9] T. Oh, S. Islam, M. Mahfouz, and G. To, "A low-power CMOS piezoelectric transducer based energy harvesting circuit for wearable sensors for medical applications," *Journal of Low Power Electronics and Applications*, vol. 7, no. 4, p. 33, December 2017.

[10] A. Toprak and O. Tigli, "MEMS scale PVDF-TrFE-based piezoelectric energy harvesters," *Journal of Microelectro-mechanical Systems*, vol. 24, no. 6, pp. 1989-1997, December 2015.

[11] Y. Zhang, T. Wang, A. Luo, Y. Hu, X. Li, and F. Wang, "Micro electrostatic energy harvester with both broad bandwidth and high normalized power density," *Applied Energy*, vol. 212, pp. 362-371, February 2018.

[12] G. Janusas, S. Ponelyte, A. Brunius, A. Guobiene, I. Prosycevas, A. Vilkauskas, *et al*., "Periodical microstructures based on novel piezoelectric material for biomedical applications," *Sensors*, vol. 15, no. 12, pp. 31699-31708, December 2015.

[13] S. Saadon and O. Sidek, "Micro-electro-mechanical system (MEMS)-based piezoelectric energy harvester for ambient vibrations," *Procedia Social and Behavioral Sciences*, vol. 195, pp. 2353-2362, July 2015.

[14] M. Safaei, R. M. Meneghini, and S. R. Anton, "Energy harvesting and sensing with embedded piezoelectric ceramics in knee implants," *IEEE/ASME Trans. on Mechatronics*, vol. 23, no. 2, pp. 864-874, April 2018.

[15] P. Pillatsch, E. M. Yeatman, and A. S. Holmes, "A piezoelectric frequency up-converting energy harvester with rotating proof mass for human body applications," *Sensors and Actuators A: Physical*, vol. 206, pp. 178-185, February 2014.

[16] S. K. Ghosh and D. Mandal, "High-performance bio-piezoelectric nanogenerator made with fish scale," *Applied Physics Letters*, vol. 109, no. 10, p. 103701, August 2016.

[17] Y. Jia and A. A. Seshia, "Power optimization by mass tuning for MEMS piezoelectric cantilever vibration energy harvesting," *Journal of Microelectromechanical Systems*, vol. 25, no. 1, pp. 108-117, November 2015.

[18] S. S. Won, M. Sheldon, N. Mostovych, J. Kwak, B. S. Chang, C. W. Ahn, *et al*., "Piezoelectric poly (vinylidene fluoride trifluoroethylene) thin film-based power generators using paper substrates for wearable device applications," *Applied Physics Letters*, vol. 107, no. 20, p. 202901, November 2015.

[19] L. Parali and A. Sari, "Vibration modelling of piezoelectric actuator (PEA) using Simulink software," in *Proc. 4th Int. Conf. on Electrical and Electronic Engineering*, June 2017, pp. 153-157.

[20] Y. Hu and Z. L. Wang, "Recent progress in piezoelectric nanogenerators as a sustainable power source in self-powered systems and active sensors," *Nano Energy*, vol. 14, pp. 3-14, May 2015.

[21] B. Y. Kim, W. H. Lee, H. G. Hwang, D. H. Kim, J. H. Kim, S. H. Lee, *et al.*, "Resistive switching memory integrated with nanogenerator for self ‐ powered bioimplantable devices," *Advanced Functional Materials*, vol. 26, no. 29, pp. 5211-5221, May 2016.

[22] B. Lu, Y. Chen, D. Ou, H. Chen, L. Diao, W. Zhang, *et al*., "Ultra-flexible piezoelectric devices integrated with heart to harvest the biomechanical energy," *Scientific Reports*, vol. 5, p. 16065, November 2015.

[23] MT3608 DC Voltage Regulator Module. (March 2019). [Online]. Available: https://prom-electric.ru/media/MT3608

[24] S. Warudkar, R. Deshmukh, and V. Parihar, "Power monitoring system using microcontroller for optimum power utility in homes," *An Int. Journal of Thesis Projects and Dissertation*, vol. 1, no. 1, 2018.

[25] M. Mnati, A. V. D. Bossche, and R. Chisab, "A smart voltage and current monitoring system for three phase inverters using an android smartphone application," *Sensors*, vol. 17, no. 4, p. 872, April 2017.

[26] J. S. Furter and P. C. Hauser, "Interactive control of purpose built analytical instruments with forth on microcontrollers-A tutorial," *Analytica Chimica Acta*, vol. 1058, pp. 18-28, June 2018.

[27] D. Artanto, M. P. Sulistyanto, I. D. Pranowo, and E. E. Pramesta, "Drowsiness detection system based on eye-closure using a low-cost EMG and ESP8266," in *Proc. 2nd Int. Conf. on Information Technology, Information Systems and Electrical Engineering*, November 2017, pp. 235-238.

[28] S. Pancholi and A. M. Joshi, "Portable EMG data acquisition module for upper limb prosthesis application," *IEEE Sensors Journal*, vol. 18, no. 8, pp. 3436-3443, February 2018.

[29] H. S. Ahmed and A. A. Ali, "Smart intensive care unit design based on wireless sensor network and internet of things," in *Proc.*

Al-Sadeq Int. Conf. on Multidisciplinary in IT and Communication Science and Applications, 2016, pp. 1-6.

[30] S. ThoiThoi, K. C. Kodur, and W. Arif, "Quaternion based wireless AHRS data transfer using nRF24L01 and HC-05," in *Proc. Int. Conf. on Microelectronics, Computing and Communications*., July 2016, pp. 1-6.

[31] nRF24 Series. (March 19, 2019). [Online]. Available: https://www.nordicsemi.com/Products/Low-power-short-range-wireless/nRF24-series

[32] N. B. Linsangan, D. L. P. Bagtas, R. T. Itchon, J. M. L. Reyes, G. M. Suarez, and R. G. Maramba, "Offline-based clicker using Gaussian frequency shift keying and arduino NRF24L01," in *Proc. IEEE 9th International Conference on Humanoid, Nanotechnology, Information Technology, Communication and Control, Environment and Management*, December 2017, pp. 1-5.

[33] Z. Chen, C. Hu, J. Liao, and S. Liu, "Protocol architecture for wireless body area network based on nRF24L01," in *Proc. IEEE International Conference on Automation and Logistics*, September 2008, pp. 3050-3054.

[34] N. Mahzan, A. M. Omar, L. Rimon, S. M. Noor, and M. Rosselan, "Design and development of an arduino based data logger for photovoltaic monitoring system," *Int. J. Simul. Syst. Sci. Technol*., vol. 17, pp. 15.1-15.5, 2017.

[35] Murata. (February 2019). [Online]. Available: https://www.murata.com/en-global/products/sound/diaphragm

[36] S. diode. (May 2019). Schottky barrier rectifiers. [Online]. Available: http://pdf.datasheetcatalog.com/datasheet/bytes/SR260.pdf

[37] M. F. Mahmood, S. L. Mohammed, and S. K. Gharghan, "Ultrasound sensor-based wireless power transfer for low-power medical devices," *Journal of Low Power Electronics and Applications*, vol. 9, no. 3, p. 20, July 2019.

[38] Y. Ye and K. W. E. Cheng, "Modeling and analysis of series–parallel switched-capacitor voltage equalizer for battery/supercapacitor strings," *IEEE Journal of Emerging and Selected Topics in Power Electronics*, vol. 3, no. 4, pp. 977-983, December 2015.

Copyright © 2020 by the authors. This is an open access article distributed under the Creative Commons Attribution License (CC BY-NC-ND 4.0), which permits use, distribution and reproduction in any medium, provided that the article is properly cited, the use is non-commercial and no modifications or adaptations are made.

Mustafa Falah Mahmood received her B.Sc. in Medical Instrumentation Techniques Eng. from Middle Technical University, Iraq in 2005. He is with the Department of Medical Instrumentation Engineering Techniques, Electrical Engineering Technical College, Middle Technical University, Baghdad-Iraq, as Technical Engineer. Currently, He studies M.Tech. in Medical Instrumentation Engineering Techniques, from Electrical Engineering Technical College, Baghdad-Iraq. His research Battery-free wearable vital signs monitoring system based on energy harvesting technique.

Saleem Lateef Mohammed received his B.Sc. in Electrical and Electronics from the Saraievo University, Eng. Bosna in 1986, his M.Sc. in Electrical and Electronics Eng. from Belgrad University, Serbia in 1988. He is with the Department of Medical Instrumentation Engineering Techniques, Electrical Engineering Technical College, Middle Technical University, Baghdad-Iraq, as Asst. Professor. His research interests include wireless sensor networks, biomedical sensors, microcontroller applications, and jamming on direct sequence spread spectrums.

Sadik Kamel Gharghan received his B.Sc. in Electrical and Electronics Eng. from the University of Technology, Iraq in 1990, his MSc. in Communication Eng. from the University of Technology, Iraq in 2005, and his Ph.D. in Communication Eng. from the University Kebangsaan Malaysia (UKM), Malaysia in 2016. He is with the Department of Medical Instrumentation Engineering Techniques, Electrical Engineering Technical College, Middle Technical University, Baghdad-Iraq, as Prof. His research interests include, energy-efficient wireless sensor networks, biomedical sensors, microcontroller applications, WSN Localization based on artificial intelligence techniques and optimization algorithms, indoor and outdoor pathloss modeling, wireless power transfer, and jamming on direct sequence spread spectrums.